Chinese Journal of Natural Medicines

Yanggan Jiangmei Formula alleviates hepatic inflammation and lipid accumulation in non-alcoholic steatohepatitis by inhibiting the NF-κB/NLRP3 signaling pathway

Yuanyuan WU, Jingwen ZHOU, Xinchen ZUO, Yufeng KUANG, Lixia SUN, Xiaolong ZHANG

Citation: Yuanyuan WU, Jingwen ZHOU, Xinchen ZUO, Yufeng KUANG, Lixia SUN, Xiaolong ZHANG, Yanggan Jiangmei Formula alleviates hepatic inflammation and lipid accumulation in non-alcoholic steatohepatitis by inhibiting the NF-κB/NLRP3 signaling pathway, Chinese Journal of Natural Medicines, 2024, 22(3), 224-234. doi: 10.1016/S1875-5364(24)60595-9.

View online: https://doi.org/10.1016/S1875-5364(24)60595-9

Available online at www.sciencedirect.com
ScienceDirect
Chinese Journal of Natural Medicines 2024, **22**(3): 224-234
doi: 10.1016/S1875-5364(24)60595-9
Chinese Journal of Natural Medicines

•Original article•

Yanggan Jiangmei Formula alleviates hepatic inflammation and lipid accumulation in non-alcoholic steatohepatitis by inhibiting the NF-κB/NLRP3 signaling pathway

WU Yuanyuan[1, 2Δ], ZHOU Jingwen[1Δ], ZUO Xinchen[1, 2], KUANG Yufeng[1, 2], SUN Lixia[1, 2*], ZHANG Xiaolong[2*]

[1] *The First Clinical Medical College, Nanjing University of Chinese Medicine, Nanjing 210023, China;*
[2] *The Affiliated Hospital of Nanjing University of Chinese Medicine, Jiangsu Province Hospital of Chinese Medicine, Nanjing 210029, China*

Available online 20 Mar., 2024

[ABSTRACT] The role of NF-κB and the NLRP3 inflammasome in the chronic inflammatory microenvironment of non-alcoholic steatohepatitis (NASH) has been posited as crucial. The Yanggan Jiangmei Formula (YGJMF) has shown promise in ameliorating hepatic steatosis in NASH patients, yet its pharmacological mechanisms remain largely unexplored. This study was conducted to investigate the efficacy of YGJMF in NASH and to elucidate its pharmacological underpinnings. To simulate NASH both *in vivo* and *in vitro*, high-fat-diet (HFD) rats and HepG2 cells stimulated with free fatty acids (FFAs) were utilized. The severity of liver injury and lipid deposition was assessed using serum indicators, histopathological staining, micro-magnetic resonance imaging (MRI), and the liver-to-muscle signal intensity ratio ($SIR_{L/M}$). Furthermore, a combination of enzyme-linked immunosorbent assay (ELISA), immunohistochemistry (IHC), immunofluorescence, real-time quantitative polymerase chain reaction (RT-qPCR), and Western blotting analyses was employed to investigate the NF-κB/NLRP3 signaling pathway and associated cytokine levels. The results from liver pathology, MRI assessments, and biochemical tests in rat models demonstrated YGJMF's significant effectiveness in reducing liver damage and lipid accumulation. Additionally, YGJMF markedly reduced hepatocyte inflammation by downregulating inflammatory cytokines in both liver tissue and serum. Furthermore, YGJMF was found to disrupt NF-κB activation, consequently inhibiting the assembly of the NLRP3 inflammasome in both the *in vitro* and *in vivo* models. The preliminary findings of this study suggest that YGJMF may alleviate hepatic steatosis and inhibit the NF-κB/NLRP3 signaling pathway, thereby exerting anti-inflammatory effects in NASH.

[KEY WORDS] Non-alcoholic steatohepatitis; Nuclear factor kappa B; NLRP3 inflammasome; Yanggan Jiangmei Formula
[CLC Number] R965 **[Document code]** A **[Article ID]** 2095-6975(2024)03-0224-11

Introduction

Non-alcoholic steatohepatitis (NASH), a key manifestation of metabolic associated fatty liver disease (MAFLD), has a global prevalence of approximately 25%, showing an upward trend over the years [1]. Despite extensive research, no specific agent has been conclusively proven effective for NASH to date [2]. Widely accepted theories, including the 'two-hit' and 'multi-hit' hypotheses, underscore chronic inflammation as a primary contributor to NASH progression through pro-inflammatory insults and associated microenvironment changes [3]. Therefore, understanding the mechanisms that mitigate hepatic inflammation is essential for developing novel therapeutic approaches to prevent and treat steatohepatitis.

Nuclear factor kappa B (NF-κB)-related inflammatory signaling is recognized as a classic pathway in inflammation and a pivotal mechanism in NASH progression [4]. Studies have noted an upregulation in the NF-κB-related inflammatory response due to the activation of the inflammasome-proinflammatory cytokine axis in NASH [5]. The interaction between NF-κB and the NOD-like receptor protein 3 (NLRP3) inflammasome, key in cellular inflammatory responses, plays a crucial role in producing inflammatory cytokines [6]. NLRP3 inflammasome activation requires both

[Received on] 23-May-2023
[Research funding] This work was supported by the National Natural Science Foundation of China (No. 8200151236), the Postgraduate Research Practice Innovation Program of Jiangsu Province (No. KYCX22_1903) and the Outstanding Clinical Talents of Traditional Chinese Medicine in Jiangsu Province (No. 18, Jiangsu Science and Education of Traditional Chinese Medicine [2017]).
[*]**Corresponding author]** E-mails: zynkslx@njucm.edu.cn (SUN Lixia); chufangzai1234@163.com (ZHANG Xiaolong)
[Δ]These authors contributed equally to this work.
These authors have no conflict of interest to declare.

priming and assembly signals [7]. NF-*κ*B-mediated priming signals are essential for NLRP3 inflammasome activation. Endogenous cytokines or microbial components can activate NF-*κ*B, leading to increased levels of NLRP3, pro-IL-1β, and pro-IL-18 [8]. NF-*κ*B activation facilitates the assembly of the NLRP3 inflammasome, triggering caspase-1 activation and subsequent production of mature IL-1β and IL-18 [9]. These processes exacerbate hepatocyte inflammation and liver injury. Recent research emphasizes the importance of the NLRP3 inflammasome as a key promoter of liver inflammation in NASH [10]. Inhibiting the NLRP3 inflammasome by blocking the NF-*κ*B signaling pathway may ameliorate NASH pathophysiology [11], suggesting that targeting the NF-*κ*B/NLRP3 pathway could be a promising strategy in NASH prevention and treatment.

Recent years have also highlighted challenges in NASH drug development, particularly concerning side effects and drug dependence [12]. Concurrently, there is growing interest in the role of herbal remedies from Traditional Chinese Medicine (TCM) in modulating inflammatory responses, especially in NASH [13]. The Yanggan Jiangmei Formula (YGJMF), an experiential blend of six herbs (*Ligustrum lucidum* Ait., *Ophiopogon japonicus* (Linn. f.) Ker-Gawl., *Lycium barbarum* L., *Forsythia suspensa* (Thunb.) Vahl, *Atractylodes macrocephala* Koidz., and *Glycyrrhiza uralensis* Fisch.), formulated by TCM expert Professor JIN Shi, has long been used clinically as an effective liver protectant [14, 15]. Although YGJMF has shown promising efficacy in improving liver function in NASH patients, its underlying mechanisms remain to be elucidated.

This study aims to delineate the specific molecular mechanisms by which YGJMF alleviates liver inflammation and prevents NASH progression. The focus is on verifying YGJMF's regulatory effects on the NF-*κ*B/NLRP3 signaling pathway in the treatment of NASH, particularly in the context of inflammatory response.

Materials and Methods

Reagents and antibodies

Antibodies against NF-*κ*B p65 (Catalog No. 8242), phospho-NF-*κ*B p65 (Catalog No. 3033), I*κ*B-α (Catalog No. 4812), caspase 1 (Catalog No. 83383), GAPDH (Catalog No. 5174), and *β*-actin (Catalog No. 4970) were sourced from Cell Signaling Technology (Danvers, USA). The NLRP3 antibody (Catalog No. ab263899) and pro-caspase 1 antibody (Catalog No. ab179515) were acquired from Abcam (Cambridge, UK). Additionally, antibodies for ASC (Catalog No. WL02462), pro-IL-1β (Catalog No. WL02257), IL-1β (Catalog No. WL00891), and IL-18 (Catalog No. WL01127) were procured from Wanleibio (Shenyang, China).

Animals

Thirty-six SPF-grade male Sprague-Dawley (SD) rats, aged 6 to 8 weeks, were obtained from the Zhejiang Academy of Medical Sciences (License No. SCXK [Zhe] 2019-0002). The experimental protocols were approved by the Committee on Laboratory Animal Care of Nanjing University of Chinese Medicine (No. A210303), adhering to the National Institutes of Health (United States) guidelines for humane care.

Prior to experimentation, rats were housed under standard conditions with unrestricted access to water and food, undergoing a one-week adaptation period. The rats were randomly divided into six groups: Control, Vehicle, Essentiale, YGJM-Low, YGJM-Middle, and YGJM-High. The NASH model was induced through a 12-week HFD regimen [16]. Subsequently, each group received daily intragastric administration of their respective treatments for four weeks, calculated based on the body surface area ratio: Control and Vehicle groups received normal saline; the Essentiale group was given Essentiale (120 mg·kg^{-1}, Sanofi #H20059010, Beijing, China) [17] the YGJM-Low, YGJM-Middle, and YGJM-High groups received YGJMF at dosages of 3.25, 6.5, and 13 g·kg^{-1}, respectively. Post-treatment, blood, and liver tissues were collected, and the rats were humanely euthanized.

YGJMF preparation

The YGJMF comprises six types of distinct herbal components: *Jiunvzhenzi* (dried mature seeds of *Ligustrum lucidum*, Batch No. 21031413), *Maidong* (root of *Ophiopogon japonicus*, Batch No. 21012023), *Gouqizi* (fruit of *Lycium barbarum*, Batch No. 20122323), *Lianqiao* (fruit of *Forsythia suspensa*, Batch No. 20010083), *Fuchaobaizhu* (rhizoma of *Atractylodes macrocephala*, Batch No. 21012083), and *Zhigancao* (roots and rhizoma *Glycyrrhiza uralensis*, Batch No. 21031423), with the ratio of 15 ∶ 15 ∶ 12 ∶ 15 ∶ 10 ∶ 6. Isodose granules of these TCM materials, provided by Jiangyin Tianjiang Pharmaceutical Co., Ltd., were used following quality control measures. These granules were dissolved in distilled water to create various concentrations of YGJMF for the studybased on our previous experience [15].

Preparation of drug-containing serum

Eighteen healthy male SD rats were maintained under standard conditions and divided into six groups: Control, Vehicle, Essentiale, YGJM-Low, YGJM-Middle, and YGJM-High. The YGJM-Low, YGJM-Middle, and YGJM-High groups received YGJMF orally at doses of 3.25, 6.5, and 13 g·kg^{-1}, respectively. The Essentiale group was given 120 mg·kg^{-1} Essentiale *via* oral administration, while the Control and Vehicle groups received 0.9% normal saline (1 mL/100 g body weight) daily for 8 d. After the eighth administration, blood was collected from the rats and centrifuged to obtain serum supernatants for further analysis.

High-performance liquid chromatography (HPLC) analysis

Serum samples containing YGJMF were prepared and filtered for analysis using HPLC. The HPLC was conducted using a Waters E2695 high-performance liquid chromatograph from Waters Co. (Massachusetts, USA). Standard compounds including salidroside (Catalog No. 10338-51-9), chlorogenic acid (Catalog No. 327-97-9), forsythoside A (Catalog No. 79916-77-1), liquiritin (Catalog No. 551-15-5), specnuezhenide (Catalog No. 39011-92-2), quercetin (Catalog No. 117-39-5), atractylenolide III (Catalog No. 73030-71-4), methylophiopogonanone A (Catalog No. 74805-92-8),

and glycyrrhetinic acid (Catalog No. 471-53-4) were obtained from Chengdu Herbpurify Co., Ltd. (Chengdu, China). These compounds were utilized to create a control solution for the HPLC analyses, as illustrated in Supplementary Fig. 2.

Cell culture

The HepG2 cell line, obtained from BeNa Culture Collection (BNCC, Beijing, China), was cultured in Dulbecco's Modified Eagle's Medium (DMEM) supplied by Gibco (New York, USA). To simulate non-alcoholic steatohepatitis (NASH) *in vitro*, HepG2 cells were exposed to free fatty acids (FFAs) comprising a mixture of oleic acid and palmitoleic acid at a concentration of 1 mmol·L^{-1} (ratio 2 ∶ 1, *M*/*M*) obtained from Sigma-Aldrich (St. Louis, USA) for 24 h [18]. Pyrrolidine dithiocarbamate (PDTC), an NF-*κ*B inhibitor sourced from MedChem Express (China), was dissolved in distilled water and subsequently diluted to a concentration of 50 μmol·L^{-1}. PDTC was used to pre-treat HepG2 cells as a reference control.

Serum biochemical analysis

The serum levels of aspartate transaminase (AST), alanine transaminase (ALT), triglyceride (TG), total cholesterol (TC), high-density lipoprotein (HDL), low-density lipoprotein (LDL), gamma-glutamyl transpeptidase (GGT), and alkaline phosphatase (ALP) were quantified using biochemical marker assay kits from Nanjing Jiancheng Bioengineering Institute (Nanjing, China). The assays were performed using an automatic blood chemical analyzer from Hitachi (Tokyo, Japan).

Histological and immunohistochemical analysis

Liver tissue samples were sectioned into 5-mm slices and mounted onto slides (Sigma-Aldrich, USA). The slides were then processed for hematoxylin and eosin (H&E) staining and Masson's trichrome staining, as well as NF-*κ*B and NLRP3 immunohistochemistry (IHC), using kits from Sangon Biotech (Shanghai, China). These procedures aimed to assess the extent of hepatic pathological changes. The Non-Alcoholic Fatty Liver Disease (NAFLD) Activity Score (NAS) was evaluated and calculated for liver sections stained with H&E [19].

Oil Red O staining

Frozen liver samples were cut on a 3050 S cryostat microtome (Leica Microsystems, Wetzlar, Germany) and mounted on microscope slides, stained by an Oil Red O staining kit (Beijing Leagene Biotechnology Co., Ltd., Beijing, China) and viewed under light microscope (Leica Microsystems, Wetzlar, Germany).

Immunofluorescence

Cell samples were first fixed adequately and then blocked in 4% bovine serum albumin. Subsequently, they were incubated with primary antibodies derived from rabbit and fluorescein isothiocyanate (FITC)-conjugated secondary antibodies. For nuclear DNA staining, 4,6-diamidino-2-phenylindole (DAPI, Southern Biotech, Alabama, USA) was used. The stained cells were visualized using an inverted fluorescence microscope from ZEISS (Germany) at 20× magnification.

Real-time quantitative polymerase chain reaction

Total RNA was extracted from both liver tissues and cell samples for real-time quantitative polymerase chain reaction (RT-qPCR) analysis. The expression level of *β*-actin messenger RNA (mRNA) served as an internal control. Specific primers for NF-*κ*B, I*κ*B-α, NLRP3, ASC, caspase 1, IL-1β, and *β*-actin were designed for this purpose. The quantitative primers used for amplification are detailed in Table 1 (not provided in the text). This RT-qPCR analysis aimed to quantitatively evaluate the gene expression levels related to the inflammatory signaling pathways under investigation (Table 1).

Enzyme-linked immunosorbent assay (ELISA)

Following centrifugation of the blood at 3500 r·min^{-1} for 20 min, a supernatant was obtained. Additionally, liver tissue or cell samples were homogenized in phosphate-buffered saline (PBS) and subsequently centrifuged. The levels of TNF-α (Catalog No. F3056-A), IL-6 (Catalog No. F3066-A), IL-1β (Catalog No. F2923-A), and IL-18 (Catalog No. F3070-A)

Table 1 Primers for quantitative polymerase chain reaction

Gene	Forward	Reverse
NF-κB (Rat)	AGAGCAACCGAAACAGAGAGG	TTTGCAGGCCCCACATAGTT
IκB-α (Rat)	CAAGTACCCGGATACAGCAG	ACACAGTCATCGTAGGGCAA
NLRP3 (Rat)	GAGCTGGACCTCAGTGACAATGC	ACCAATGCGAGATCCTGACAACAC
ASC (Rat)	TGGAGTCGTATGGCTTGGA	TGTCCTTCAGTCAGCACACT
Caspase-1 (Rat)	ACTCGTACACGTCTTGCCCTC	CTGGGCAGGCAGCAAATTC
IL-1β (Rat)	CACCTCTCAAGCAGAGCACAG	GGGTTCCATGGTGAAGTCAAC
β-Actin (Rat)	TGCTATGTTGCCCTAGACTTCG	GTTGGCATAGAGGTCTTTACGG
NF-κB (human)	AACAGAGAGGATTTCGTTTCCG	TTTGACCTGAGGGTAAGACTTCT
IκB-α (human)	TGGTCAGTGCCTTTTCTTCAT	GGAGTACGAGCAGATGGTCAA
NLRP3 (human)	ACAAGCCACCTCACTTCCAG	CCAACCACAATCTCCGAATG
ASC (human)	GCTGGAGAACCTGACCGC	CTCCAGAGCCCTGGTGCG
Caspase-1 (human)	GTTTCTTGGAGACATCCCAC	CTTCACTTCCTGCCCACAG
IL-1β (human)	TTCGACACATGGGATAACGAGG	TTTTTGCTGTGAGTCCCGGAG
β-Actin (human)	GTCATTCCAAATATGAGATGCGT	GCTATCACCTCCCCTGTGTG

Gene sequences (5' to 3')

in the supernatants from liver tissue, serum, and cells were quantified using ELISA kits provided by FANKEW (Shanghai, China).

Western blotting assay

Cell lysates and liver tissues, treated with YGJMF for 48 h, were homogenized on ice and centrifuged to extract the supernatant. Proteins were then transferred onto nitrocellulose membranes (Bio-Rad, California, USA). After blocking in 5% skim milk, the membranes were incubated with rabbit-derived primary antibodies overnight, followed by incubation with horseradish peroxidase-conjugated secondary antibodies. The immunoreactive bands were visualized using enhanced chemiluminescence (Bio-Rad).

Micro-magnetic resonance imaging (MRI)

Micro-MRI of livers was performed using a Bruker Pharma Scan equipped with a 7.0T superconducting magnet. The average signal magnitude and values were acquired by manually segmenting the liver from MRI images. The liver signal magnitude was normalized to the signal magnitude of the surrounding erector spinae muscles, termed the Liver-to-Muscle Signal Intensity Ratio ($SIR_{L/M}$). $SIR_{L/M}$ for each image was calculated using ParaVision 5 software (Bruker) and Amira imaging PC-based software for data analysis [20].

Statistical analysis

Data were expressed as mean ± standard deviation. Analysis of variance (ANOVA) was employed for multiple data set comparisons, while a *t*-test was used for two-group comparisons. A *P*-value of < 0.05 was considered statistically significant. SPSS v23.0 and GraphPad Prism v8.0 software were utilized for data analysis.

Results

YGJMF relieved hepatic injury and lipid accumulation in HFD-fed rats

The liver-protective effects of the YGJMF were investigated in a HFD-induced rat model. Throughout the feeding period, as expected, the body weight of rats in each group steadily increased. Post-treatment with varying concentrations of YGJMF, there was a noted reduction in both liver weight and the liver-to-body weight ratio. However, these changes were not statistically significant when compared with the Vehicle group, as detailed in Supplementary Figs. 1B−1D. Biochemical analyses were conducted to assess YGJMF's impact on liver injury. As illustrated in Fig.1, YGJMF treatment significantly reduced serum levels of AST, ALT, TG, TC, LDL, GGT, and ALP, while increasing HDL levels compared with the Vehicle group (Figs. 1A−1H). These results indicate that YGJMF effectively mitigates liver injury and lowers serum lipid levels in HFD-fed rats.

YGJMF ameliorated HFD-induced liver injury and lipid deposition

The YGJMF demonstrated significant efficacy in mitig-

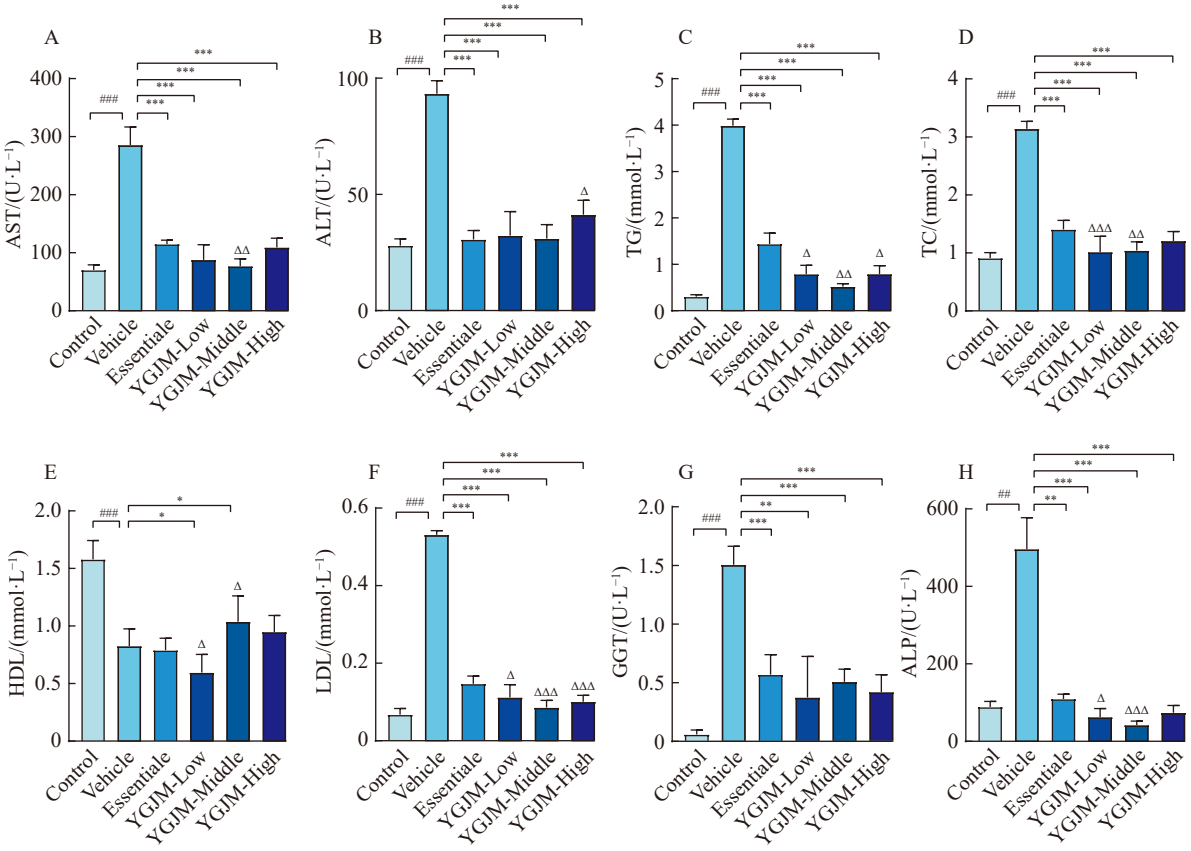

Fig. 1 Effects of YGJMF on the biochemical parameters in serum of HFD-fed rats. (A) AST. (B) ALT. (C) Serum TG. (D) total cholesterol (TC). (E) HDL. (F) LDL. (G) GGT and (H) ALP in each group. Data are represented as mean ± SD (n = 6). $^{\#\#}P < 0.01$, $^{\#\#\#}P < 0.001$ *vs* Control; $^{*}P < 0.05$, $^{**}P < 0.01$, $^{***}P < 0.001$ *vs* Vehicle; $^{\triangle}P < 0.05$, $^{\triangle\triangle}P < 0.01$, $^{\triangle\triangle\triangle}P < 0.001$ *vs* Essentiale.

ating liver injury and lipid deposition in a HFD-induced rat model, as evidenced by the data presented in Fig. 2A. Visual inspection revealed notable fat accumulation on the liver surface in the Vehicle group, characterized by a dull yellow appearance and blurred edges. In contrast, livers from the Essentiale and YGJMF-treated groups displayed a marked improvement, showing reduced fat and a deeper red color. This was particularly evident in the YGJM-High group, suggesting that YGJMF considerably reduces hepatic lipid accumulation compared to the Vehicle group (Fig. 2A).

Hematoxylin and eosin (H&E) staining (Fig. 2B, upper panel) demonstrated a clear reduction in lipid droplets and inflammatory infiltration in the YGJMF-treated groups, indicating the formula's effectiveness in alleviating steatosis, hepatic necrosis, hepatocyte ballooning, and lobular inflammation caused by HFD. Additionally, the associated hepatic lesions and triglyceride (TG) levels, along with the NAS, were also reduced (Figs. 2A−2B). Oil Red O staining revealed that YGJMF treatment notably prevented the exacerbation of hepatic lipid accumulation, with significant improvements observed in all treatment groups compared to the Vehicle group (Fig. 2B, middle panel). Furthermore, Masson's trichrome staining indicated fibrous hyperplasia in the Vehicle group, while YGJMF treatment resulted in a reduction of fibroblastic deposition in liver tissue (Fig. 2B, lower panel). These findings underscore YGJMF's capacity to diminish excessive lipid accumulation and improve hepatic injury in HFD-induced rats.

Micro-MRI, a tool for evaluating the severity of hepatic damage and elucidating early morphological alterations (Fig. 2C) based on our previous experience [20], further substantiated the therapeutic potential of YGJMF. Liver MRI, increas-

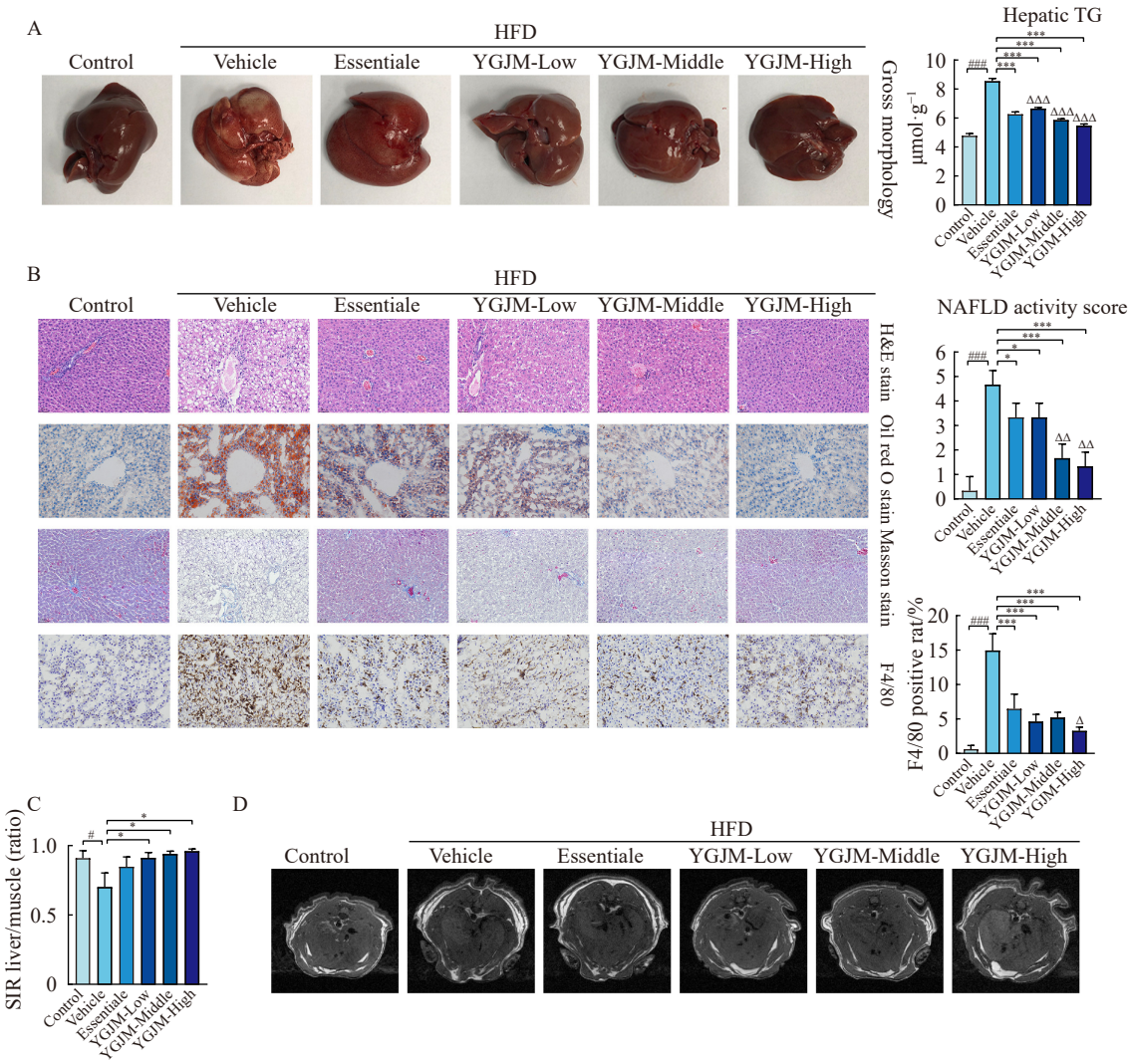

Fig. 2 Effects of YGJMF on macroscopic and microscopic hepatic architecture in HFD-fed rats and ameliorated HFD-induced hepatic tissue injury and lipid metabolism. Representative images of (A) macroscopic features of liver morphology and TG level in THE liver; (B) H&E staining (NAS), Oil Red O staining, Masson staining, and IHC of F4/80 in liver pathological sections of rats in each group. Magnification × 200; (C−D) $SIR_{L/M}$ values of each slice of micro-MRI and representative image in each group. Data are represented as mean ± SD (n = 6). $^{\#}P < 0.05$, $^{\#\#\#}P < 0.001$ *vs* Control; $^{*}P < 0.05$, $^{***}P < 0.001$ *vs* Vehicle; $^{\triangle\triangle}P < 0.01$ $^{\triangle\triangle\triangle}P < 0.001$ *vs* Essentiale.

ingly used in diagnosing liver diseases, including NASH, offers a quantitative approach to characterizing subtle structural changes in liver injury [21]. The $SIR_{L/M}$ is recognized as a noninvasive diagnostic tool for liver diseases, correlating with inflammatory activity and the severity of NASH [22, 23]. In this study, $SIR_{L/M}$ values decreased in the Vehicle group but significantly increased in the YGJMF treatment groups, highlighting YGJMF's effectiveness in liver protection (Fig. 2D).

YGJMF decreased HFD-induced inflammatory responses

Immunostaining indicated an increased presence of macrophages in the livers of HFD-induced rats, a hallmark of inflammation. YGJMF treatment effectively suppressed the expression of the macrophage surface marker F4/80 (Fig. 2B), suggesting that YGJMF alleviates liver inflammation and macrophage infiltration. This is a critical observation, as macrophage infiltration is a key feature of inflammatory responses in liver diseases. Hepatocyte injuries in NASH are known to induce several pro-inflammatory cytokines, including IL-1β, IL-18, TNF-α, and IL-6 [24, 25]. These cytokines were measured to assess the inflammatory state in the rat model (Figs. 3A−3H). The YGJMF treatment groups showed significant downregulation in the levels of these pro-inflammatory cytokines in both liver tissue and serum compared to the Vehicle group. Notably, the YGJM-Middle group exhib-

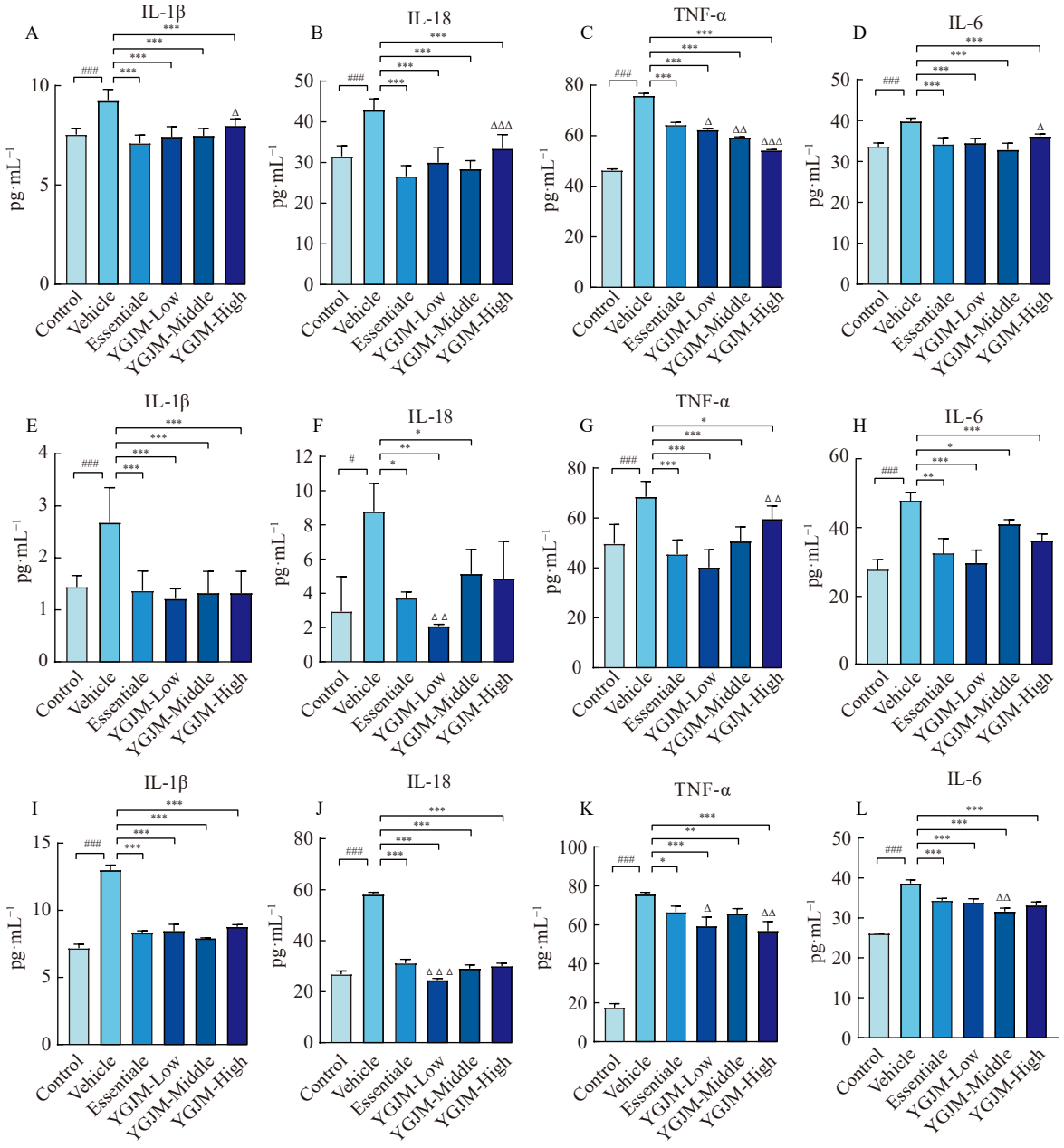

Fig. 3 YGJMF lessened inflammatory responses in NASH. Levels of IL-1β, IL-18, TNF-α, and IL-6 of liver tissue (A−D), serum (E−H), and HepG2 cells (I−L) in each group were detected by ELISA. Data are represented as mean ± SD (n = 3). $^{\#}P < 0.05$, $^{\#\#\#}P < 0.001$ *vs* Control; $^{*}P < 0.05$, $^{**}P < 0.01$ and $^{***}P < 0.001$ *vs* Vehicle; $^{\triangle}P < 0.05$, $^{\triangle\triangle}P < 0.01$, $^{\triangle\triangle\triangle}P < 0.001$ *vs* Essentiale.

ited the most significant improvement in the expression of hepatic inflammatory cytokines, while the YGJM-Low group demonstrated the most effective reduction in serum cytokine levels. The observed decrease in pro-inflammatory cytokines suggests that YGJMF ameliorates liver injury by attenuating the inflammatory response. This effect is crucial, as chronic inflammation is a significant driver of NASH progression. The data imply that YGJMF may exert its therapeutic effects by modulating the inflammatory milieu in the liver, highlighting its potential as an effective intervention for NASH characterized by inflammation and macrophage infiltration.

YGJMF suppressed HFD-induced liver injury by downregulating NF-κB/NLRP3 signaling pathway in vivo

The YGJMF appears to exert its therapeutic effects on HFD-induced liver injury by targeting the NF-κB/NLRP3 signaling pathway, as evidenced by IHC, Western blotting, and RT-qPCR analyses. IHC analysis of liver tissue revealed an increased expression of NF-κB and NLRP3 in the Vehicle group. In contrast, YGJMF treatment resulted in reduced expression of both NF-κB and NLRP3 in a dose-dependent manner. This observation suggests that YGJMF mitigates liver inflammation and injury by modulating these key inflammatory mediators (Fig. 4A). Western blotting analysis further supported these findings, showing inhibited activation of the NF-κB/NLRP3 signaling pathway in the YGJMF-treated liver. Specifically, there was a reduction in the expression levels of NF-κB, NLRP3, ASC, caspase-1, IL-1β, and IL-18. This inhibition indicates that YGJMF effectively disrupts the cascade of events leading to inflammation in NASH (Fig. 4B). Consistent with the protein expression trends, RT-qPCR analysis demonstrated a significant downregulation in the relative mRNA levels of components of the NF-κB/NLRP3 signaling pathway following YGJMF treatment, particularly in the YGJM-High group. This gene expression data further corroborates the inhibitory effect of YGJMF on this inflammatory signaling pathway (Figs. 4C−4H). These results collectively suggest a direct correlation between the protective effects of YGJMF against HFD-induced liver steatosis and the downregulation of the NF-κB/NLRP3 signaling pathway. By targeting this pathway, YGJMF effectively reduces the production of key inflammatory cytokines and mediators, thereby mitigating liver injury and inflammation. This mechanism of action highlights the potential of YGJMF as a therapeutic agent in managing NASH, particularly in cases where inflammation plays a central role.

YGJMF alleviated lipid deposition and downregulated NF-κB/NLRP3 signaling pathway in FFA-induced HepG2 cells

The YGJMF demonstrated significant efficacy in reducing lipid accumulation and modulating the NF-κB/NLRP3 signaling pathway in FFA-induced HepG2 cells, as illustrated in the presented figures and experimental data. Fig. 5A

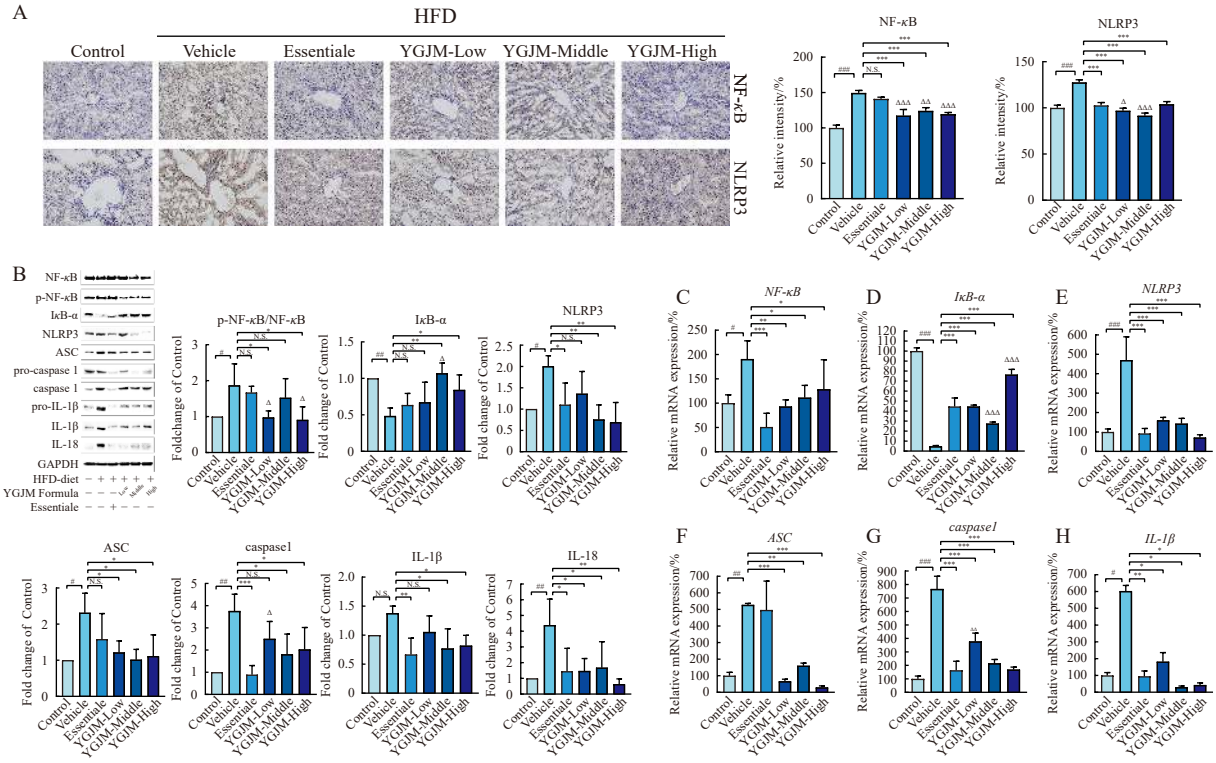

Fig. 4 YGJMF mitigated HFD-induced change of NF-κB/NLRP3 signaling pathway *in vivo*. (A) Immunohistochemical staining assay and quantitative analysis of NF-κB and NLRP3 intensity in liver. Magnification × 200. (B) The effect of YGJMF on the protein level of NF-κB, p-NF-κB, IκB-α, NLRP3, ASC, pro-caspase 1, caspase 1, pro-IL-1β, IL-1β and IL-18 in liver tissue of each group; (C−H) The effect of YGJMF on the relative messenger RNA level of *NF-κB*, *IκB-α*, *NLRP3*, *ASC*, *caspase1*, *IL-1β* in liver tissue of NASH rats. Data are represented as mean ± SD (n = 3). $^{\#}P < 0.05$, $^{\#\#\#}P < 0.001$ *vs* Control; $^{*}P < 0.05$, $^{**}P < 0.01$ and $^{***}P < 0.001$ *vs* Vehicle; $^{\triangle\triangle}P < 0.01$, $^{\triangle\triangle\triangle}P < 0.001$ vs Essentiale.

shows that FFA treatment led to the formation of macro-lipid droplets in HepG2 cells, which were notably diminished following treatment with YGJMF-medicated serum compared to the Vehicle group. Additionally, levels of pro-inflammatory cytokines were significantly lowered in FFA-induced HepG2 cells treated with YGJMF (Figs. 3I−3L). Further *in vitro* experiments validated YGJMF's influence on the NF-*κ*B/NLRP3 signaling pathway. Post-treatment with YGJMF, both protein levels and mRNA expressions of related markers in HepG2 cells showed a notable decrease (Figs. 5B−5H). Immunofluorescence studies (Figs. 5I−5O) revealed that after FFA treatment, NF-*κ*B fluorescence intensity increased, indicating activation and nuclear translocation, which were significantly restrained by YGJMF-containing serum treatment. Moreover, the visible differences in fluorescence intensities of NLRP3, ASC, caspase-1, IL-1β, and IL-18 between the Vehicle group and treatment groups indicate YGJMF's ability to inhibit the oligomerization of ASC, activation and assembly of the NLRP3 inflammasome, and subsequent caspase-1 activation and cytokine production. These results point to the NF-*κ*B/NLRP3 signaling pathway as a functional target of YGJMF. Furthermore, PDTC, an inhibitor of NF-*κ*B, was applied to identify the related mechanism. It can be concluded that YGJMF exerted the analogous anti-inflammatory effect on PDTC; that is, both of them could downregulate NLRP3 inflammasome and the related expression. According to the levels of protein and mRNA, YGJMF could downregulate the expressions of NLRP3, ASC, caspase 1, and IL-1β, like PDTC. Moreover, immunofluorescence of YGJMF also exhibited an equal improvement effect with PDTC (Fig. 6), underscoring YGJMF's role in suppressing NF-*κ*B and downstream NLRP3 signaling pathways. These findings suggest YGJMF's potential as an NF-*κ*B-inhibitor-like agent in alleviating liver inflammation.

Discussion

Addressing chronic hepatic inflammation and alleviating liver injury in non-alcoholic steatohepatitis (NASH) remains

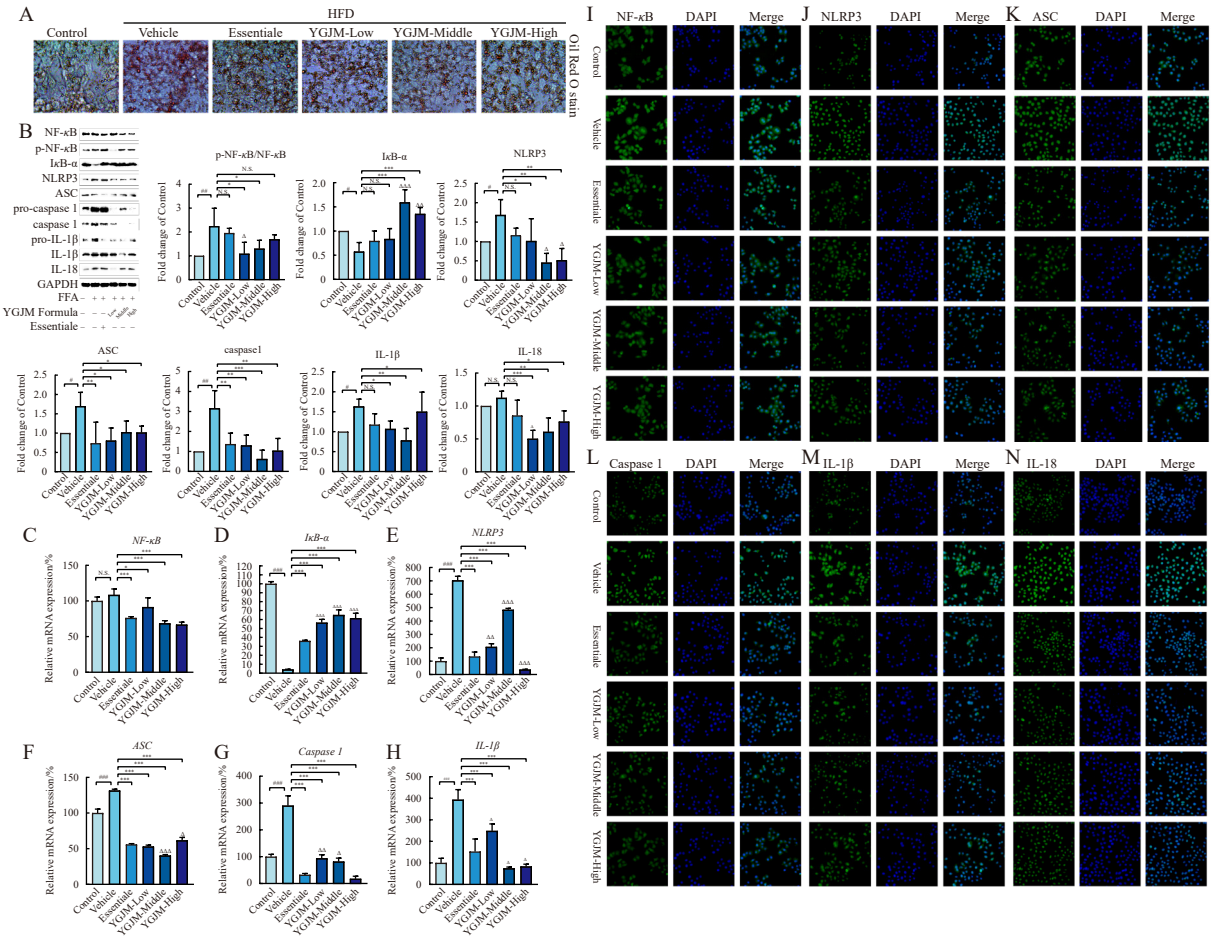

Fig. 5 YGJMF alleviated lipid deposition and attenuated expressions of NF-*κ*B/NLRP3 signaling pathway in FFA-induced HepG2 cells. (A) Oil Red O staining of cells. Magnification × 200. (B) The effects of YGJMF on the protein level of NF-*κ*B, p-NF-*κ*B, I*κ*B-*α*, NLRP3, ASC, pro-caspase 1, caspase 1, pro-IL-1β, IL-1β and IL-18 in FFA-induced HepG2 cells in each group; (C−H) The effects of YGJMF on the relative messenger RNA level of *NF-κB*, *IκB-α*, *NLRP3*, *ASC*, *caspase 1*, *IL-1β in vitro*. (I−N) YGJMF significantly suppressed the expression of NF-*κ*B, NLRP3, ASC, caspase 1, IL-1β and IL-18 in FFA-induced HepG2 cells, as determined by immunofluorescence. Magnification × 20. Data are represented as mean ± SD ($n = 3$). $^{\#}P < 0.05$, $^{\#\#}P < 0.01$ and $^{\#\#\#}P < 0.001$ *vs* Control; $^{*}P < 0.05$, $^{**}P < 0.01$ and $^{***}P < 0.001$ *vs* Vehicle; $^{\triangle}P < 0.05$, $^{\triangle\triangle}P < 0.01$, $^{\triangle\triangle\triangle}P < 0.001$ *vs* Essentiale.

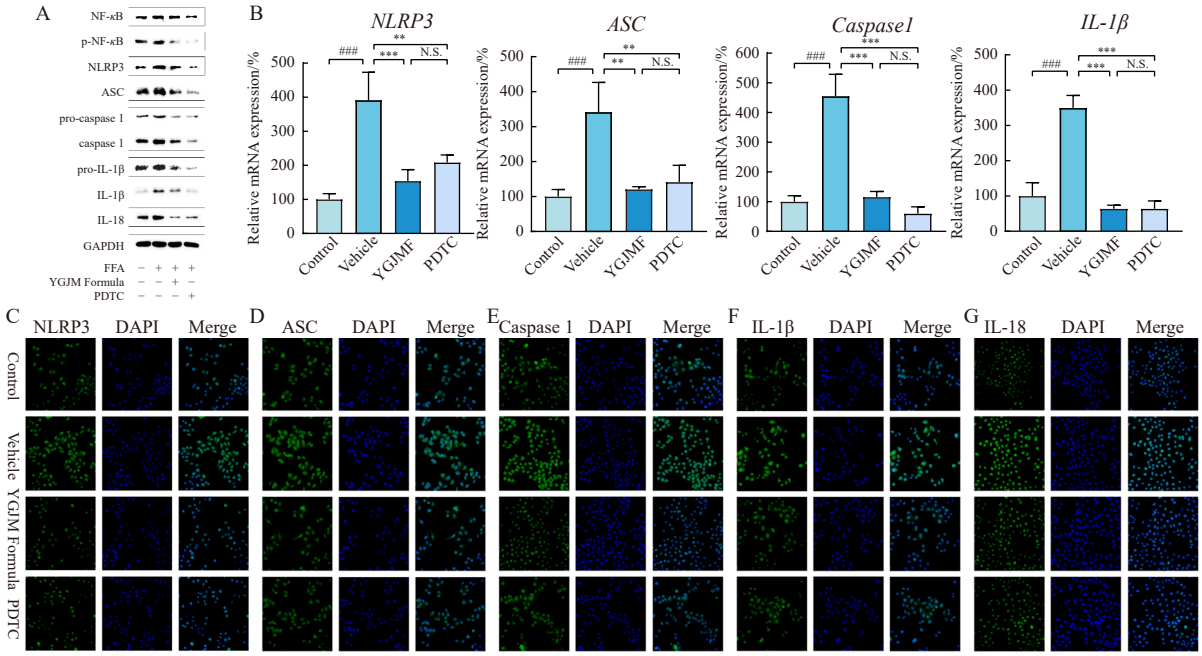

Fig. 6 YGJMF and PDTC interfered with the expression of NF-κB/NLRP3 signaling pathway in HepG2 cells induced by FFA. (A) The effects of YGJMF and PDTC on the protein level of NF-κB, p-NF-κB, NLRP3, ASC, pro-caspase 1, caspase 1, pro-IL-1β, IL-1β and IL-18 in FFA-induced HepG2 cells in each group. (B) The effects of YGJMF and PDTC on the relative messenger RNA level of *NLRP3*, *ASC*, *Caspase 1*, and *IL-1β in vitro*. (C−G) YGJMF and PDTC restrained the expression of NLRP3, ASC, caspase 1, IL-1β, and IL-18 in FFA-induced HepG2 cells, as determined by immunofluorescence. Magnification × 20. Data are represented as mean ± SD ($n = 3$). $^{\#}P < 0.05$, $^{\#\#}P < 0.01$ and $^{\#\#\#}P < 0.001$ *vs* Control; $^{*}P < 0.05$, $^{**}P < 0.01$ and $^{***}P < 0.001$ *vs* Vehicle.

a challenging clinical endeavor. Traditional Chinese Medicine (TCM) has garnered increasing interest due to its unique role in managing NASH by influencing lipid metabolism, providing liver protection, and offering anti-inflammatory benefits [13]. In this context, the YGJMF stands out as a TCM prescription noted for its high clinical safety and efficacy in liver protection and symptom improvement for NASH patients. The current study highlights that YGJMF significantly ameliorates liver injury and regulates serum lipid levels, demonstrating comparable efficacy to Essentiale, a commonly used pharmaceutical intervention in NASH treatment with widespread clinical adoption. Furthermore, the study elucidates the mechanism behind YGJMF's therapeutic action. It reveals that YGJMF mitigates steatosis and inflammation primarily by inhibiting the NF-κB/NLRP3 signaling pathway. This leads to a downregulated expression of NF-κB, which in turn restricts the nuclear translocation of NF-κB and the subsequent activation of the NLRP3 cascade response. As such, YGJMF appears to impede the activation of the NLRP3 inflammasome right from its priming step, thus manifesting its anti-inflammatory activity akin to that of an NF-κB inhibitor. This ability to alleviate liver inflammation positions YGJMF as a promising therapeutic agent in the treatment of NASH, particularly in cases where inflammation is a key pathogenic factor.

TNF-α is critical in the progression of non-alcoholic steatohepatitis (NASH) by influencing lipid metabolism regulatory molecules and inflammatory cytokines in hepatocytes [26]. It negatively impacts inflammation by inhibiting the transcription of adiponectin in adipocytes [27]. Adiponectin, a potent anti-inflammatory adipokine, suppresses hepatic production of TNF-α and IL-6 by downregulating NF-κB activity [28], thereby preventing fat accumulation and inflammation in chronic liver injury [29]. The NLRP3 signal axis, known to be involved in regulating IL-6 [30], is also influenced by TNF-α [31]. However, the role of adiponectin in the NLRP3 inflammasome remains an area for further investigation.

YGJMF alleviates hepatic steatosis and lipid accumulation in NASH by targeting multiple pathways. The progression of NASH involves increased expression of inflammatory cytokines, which activate the downstream NF-κB/NLRP3 signaling pathway, creating a feedback loop that exacerbates inflammation and lipid deposition in the liver [32]. Various lipid species play a crucial role in regulating the NLRP3 inflammasome [33], and its activation aggravates hepatic steatosis and liver inflammation, underscoring the NLRP3 inflammasome's contribution to NASH pathogenesis [34]. This inflammatory signaling can further promote lipid accumulation in the liver [35], with liver cell fat accumulation also enhancing inflammatory cytokine production, thereby exacerbating NASH [36]. Lipid deposition activates NLRP3 expression and its downstream inflammatory factors, intensifying the inflammatory response [37]. Some lipids also have key upstream roles in mediating inflammasome activation, indicating their essential functions in lipid metabolic diseases [38], including NASH [39].

NLRP3 inflammasome plays an important role in lipid deposition and inflammatory response initiation of NASH [40]. YGJMF contains several important chemical compounds that exhibit anti-lipid deposition and regulate NF-κB and NLRP3 inflammasome-related inflammatory responses in NASH. These include Salidroside [41-43], Forsythiaside [44], Ophiopogon polysaccharide [45], Lycium barbarum polysaccharides [46], Chlorogenic Acid [47], Quercetin [48], Atractylenolide III [49] and Glycyrrhetinic acid [50]. This suggests YGJMF's potential in modulating the interaction between lipid deposition and inflammatory response through multi-target selective mechanisms. Further research is needed to elucidate whether YGJMF modulates the interplay between lipid deposition and inflammatory response or operates through multi-target-selective methods. Understanding the link between lipids and inflammasome activation is crucial for developing NASH therapeutics. The specific mechanisms by which YGJMF exerts its effects in NASH, particularly in the context of inflammasome regulation and lipid metabolism, will be an important focus for future studies.

Conclusion

To conclude, the findings of this study reveal that the YGJMF effectively suppresses liver inflammation and dysregulated lipid metabolism in non-alcoholic steatohepatitis (NASH) through the inhibition of the NF-κB-related NLRP3 signaling pathway. This action results in the mitigation of NASH progression. Our research provides new insights into the therapeutic intervention of NASH using YGJMF, suggesting it as a viable option in the treatment of this condition. However, further detailed studies are warranted to comprehensively understand the relationship between YGJMF and NLRP3-related processes such as mitophagy, oxidative stress, and pyroptosis.

Supplementary Information

Supplementary data to this article can be obtained by sending E-mail to the corresponding authors.

References

[1] Powell EE, Wong VW, Rinella M. Non-alcoholic fatty liver disease [J]. *Lancet*, 2021, **397**(10290): 2212-2224.

[2] Eslam M, Sanyal AJ, George J. MAFLD: a consensus-driven proposed nomenclature for metabolic associated fatty liver disease [J]. *Gastroenterology*, 2020, **158**(7): 1999-2014. e1.

[3] Buzzetti E, Pinzani M, Tsochatzis EA. The multiple-hit pathogenesis of non-alcoholic fatty liver disease (NAFLD) [J]. *Metabolism*, 2016, **65**(8): 1038-1048.

[4] Cai D, Yuan M, Frantz DF, *et al*. Local and systemic insulin resistance resulting from hepatic activation of IKK-β and NF-κB [J]. *Nat Med*, 2005, **11**(2): 183-190.

[5] Afonina IS, Zhong Z, Karin M, *et al*. Limiting inflammation-the negative regulation of NF-κB and the NLRP3 inflammasome [J]. *Nat Immunol*, 2017, **18**(8): 861-869.

[6] Swanson KV, Deng M, Ting JP, The NLRP3 inflammasome: molecular activation and regulation to therapeutics [J]. *Nat Rev Immunol*, 2019, **19**(8): 477-489.

[7] Paik S, Kim JK, Silwal P, *et al*. An update on the regulatory mechanisms of NLRP3 inflammasome activation [J]. *Cell Mol Immunol*, 2021, **18**(5): 1141-1160.

[8] Jo EK, Kim JK, Shin DM, *et al*. Molecular mechanisms regulating NLRP3 inflammasome activation [J]. *Cell Mol Immunol*, 2016, **13**(2): 148-159.

[9] Broz P, Dixit VM. Inflammasomes: mechanism of assembly, regulation and signalling [J]. *Nat Rev Immunol*, 2016, **16**(7): 407-420.

[10] Calcagno DM, Chu A, Gaul S, *et al*. NOD-like receptor protein 3 activation causes spontaneous inflammation and fibrosis that mimics human NASH [J]. *Hepatology*, 2022, **76**(3): 727-741.

[11] Wallert M, Börmel L, Lorkowski S. Inflammatory diseases and vitamin E-what do we know and where do we go? [J]. *Mol Nutr Food Res*, 2021, **65**(1): e2000097.

[12] Younossi ZM, Loomba R, Rinella ME, *et al*. Current and future therapeutic regimens for nonalcoholic fatty liver disease and nonalcoholic steatohepatitis [J]. *Hepatology*, 2018, **68**(1): 361-371.

[13] Yao H, Qiao YJ, Zhao YL, *et al*. , Herbal medicines and nonalcoholic fatty liver disease [J]. *World J Gastroenterol*, 2016, **22**(30): 6890-6905.

[14] Gao W, Chen Q, Sun L. Professor Jin Shi's experience in the treatment of chronic hepatitis B with elevated AST [J]. *Chin J Ethnomed Ethnopharm*, 2021, **30**(20): 85-87.

[15] Wu Y, Kuang Y, Wu Y, *et al*. Yang-Gan-Jiang-Mei formula alleviates non-alcoholic steatohepatitis by inhibiting NLRP3 inflammasome through mitophagy [J]. *Biotechnol Genet Eng Rev*, 2023: 1-20.

[16] Zhu G, Chen L, Liu S, *et al*. Celecoxib-mediated attenuation of non-alcoholic steatohepatitis is potentially relevant to redistributing the expression of adiponectin receptors in rats [J]. *Heliyon*, 2022, **8**(7): e09872.

[17] Tang K, Deng Y, Zheng C, *et al*. Prevention of nonalcoholic hepatic steatosis by Shenling Baizhu Powder: involvement of adiponectin-induced inhibition of hepatic SREBP-1c [J]. *Oxid Med Cell Longev*, 2020, **2020**: 9701285.

[18] Wang Y, Chen C, Chen J, *et al*. Overexpression of NAG-1/GDF15 prevents hepatic steatosis through inhibiting oxidative stress-mediated dsDNA release and AIM2 inflammasome activation [J]. *Redox Biol*, 2022, **52**: 102322.

[19] Kleiner DE, Brunt EM, Van Natta M, *et al*. Design and validation of a histological scoring system for nonalcoholic fatty liver disease [J]. *Hepatology*, 2005, **41**(6): 1313-21.

[20] Zhou J, Zhang X, Wan L, *et al*. Zi Qi decoction alleviates liver fibrosis by inhibiting the toll-like receptor 4 (TLR4)-related nuclear factor kappa B (NF-κB) and mitogen-activated protein kinase (MAPK) signaling pathways [J]. *Med Sci Monit*, 2021, **27**: e929438.

[21] Dulai PS, Sirlin CB, Loomba R. MRI and MRE for non-invasive quantitative assessment of hepatic steatosis and fibrosis in NAFLD and NASH: clinical trials to clinical practice [J]. *J Hepatol*, 2016, **65**(5): 1006-1016.

[22] Balassy C, Feier D, Peck-Radosavljevic M, *et al*. Susceptibility-weighted MR imaging in the grading of liver fibrosis: a feasibility study [J]. *Radiology*, 2014, **270**(1): 149-158.

[23] Asanuma T, Ono M, Kubota K, *et al*. Super paramagnetic iron oxide MRI shows defective Kupffer cell uptake function in non-alcoholic fatty liver disease [J]. *Gut*, 2010, **59**(2): 258-266.

[24] de Carvalho Ribeiro M, Szabo G. Role of the inflammasome in liver disease [J]. *Annu Rev Pathol*, 2022, **17**: 345-365.

[25] Duan Y, Pan X, Luo J, *et al*. Association of inflammatory cytokines with non-alcoholic fatty liver disease [J]. *Front Immunol*, 2022, **13**: 880298.

[26] Akbari R, Behdarvand T, Afarin R, *et al*. Saroglitazar improved hepatic steatosis and fibrosis by modulating inflammatory cytokines and adiponectin in an animal model of non-alcoholic steatohepatitis [J]. *BMC Pharmacol Toxicol*, 2021, **22**(1): 53.
[27] Berg AH, Scherer PE. Adipose tissue, inflammation, and cardiovascular disease [J]. *Circ Res*, 2005, **96**(9): 939-949.
[28] Ouchi N, Walsh K. Adiponectin as an anti-inflammatory factor [J]. *Clin Chim Acta*, 2007, **380**(1-2): 24-30.
[29] Stojsavljević S, Gomerčić Palčić M, Virović Jukić L, *et al*. Adipokines and proinflammatory cytokines, the key mediators in the pathogenesis of nonalcoholic fatty liver disease [J]. *World J Gastroenterol*, 2014, **20**(48): 18070-18091.
[30] Ying Y, Zhang H, Yu D, *et al*. Gegen Qinlian decoction ameliorates nonalcoholic fatty liver disease in rats *via* oxidative stress, inflammation, and the NLRP3 signal axis [J]. *Evid-Based Compl Alt*, 2021, **2021**: 6659445.
[31] Yang Y, Sheng Y, Wang J, *et al*. , Double-negative T cells regulate hepatic stellate cell activation to promote liver fibrosis progression *via* NLRP3 [J]. *Front Immunol*, 2022, **13**: 857116.
[32] Wang Q, Ou Y, Hu G, *et al*. Naringenin attenuates non-alcoholic fatty liver disease by down-regulating the NLRP3/NF-*κ*B pathway in mice [J]. *Br J Pharmacol*, 2020, **177**(8): 1806-1821.
[33] Ralston JC, Lyons CL, Kennedy EB, *et al*. Fatty acids and NLRP3 inflammasome-mediated inflammation in metabolic tissues [J]. *Annu Rev Nutr*, 2017, **37**: 77-102.
[34] Schroder K, Tschopp J. The inflammasomes [J]. *Cell*, 2010, **140**(6): 821-832.
[35] Mirea AM, Tack CJ, Chavakis T, *et al*. IL-1 family cytokine pathways underlying NAFLD: towards new treatment strategies [J]. *Trends Mol Med*, 2018, **24**(5): 458-471.
[36] Ghezelbash B, Shahrokhi N, Khaksari M, *et al*. Protective roles of Shilajit in modulating resistin, adiponectin, and cytokines in rats with non-alcoholic fatty liver disease [J]. *Chin J Integr Med*, 2022, **28**(6): 531-537.
[37] Guan X, Shen S, Liu J, *et al*. Protective effecs of baicalin magnesium on non-alcoholic steatohepatitis rats are based on inhibiting NLRP3/Caspase-1/IL-1β signaling pathway [J]. *BMC Complement Med Ther*, 2023, **23**(1): 72.
[38] Anand PK. Lipids, inflammasomes, metabolism, and disease [J]. *Immunol Rev*, 2020, **297**(1): 108-122.
[39] Marra F, Svegliati-Baroni G. Lipotoxicity and the gut-liver axis in NASH pathogenesis [J]. *J Hepatol*, 2018, **68**(2): 280-295.
[40] Shi C, Yang H, Zhang Z. Involvement of nucleotide-binding oligomerization domain-like receptor family pyrin domain containing 3 inflammasome in the pathogenesis of liver diseases [J]. *Front Cell Dev Biol*, 2020, **8**: 139.
[41] Hu M, Zhang D, Xu H, *et al*. Salidroside activates the AMP-activated protein kinase pathway to suppress nonalcoholic steatohepatitis in mice [J]. *Hepatology*, 2021, **74**(6): 3056-3073.
[42] Zheng T, Yang X, Li W, *et al*. Salidroside attenuates high-fat diet-induced nonalcoholic fatty liver disease *via* AMPK-dependent TXNIP/NLRP3 pathway [J]. *Oxid Med Cell Longev*, 2018, **2018**: 8597897.
[43] Feng J, Chen K, Xia Y, *et al*. Salidroside ameliorates autophagy and activation of hepatic stellate cells in mice *via* NF-*κ*B and TGF-β1/Smad3 pathways [J]. *Drug Des Devel Ther*, 2018, **12**: 1837-1853.
[44] Gong L, Wang C, Zhou H, *et al*. A review of pharmacological and pharmacokinetic properties of Forsythiaside A [J]. *Pharmacol Res*, 2021, **169**: 105690.
[45] Wang X, Shi L, Wang X, *et al*. MDG-1, an *Ophiopogon* polysaccharide, restrains process of non-alcoholic fatty liver disease *via* modulating the gut-liver axis [J]. *Int J Biol Macromol*, 2019, **141**: 1013-1021.
[46] Xiao J, Liong EC, Ching YP, *et al*. *Lycium barbarum* polysaccharides protect rat liver from non-alcoholic steatohepatitis-induced injury [J]. *Nutr Diabetes*, 2013, **3**(7): e81.
[47] Miao H, Ouyang H, Guo Q, *et al*. Chlorogenic acid alleviated liver fibrosis in methionine and choline deficient diet-induced nonalcoholic steatohepatitis in mice and its mechanism [J]. *J Nutr Biochem*, 2022, **106**: 109020.
[48] Yi H, Peng H, Wu X, *et al*. The therapeutic effects and mechanisms of quercetin on metabolic diseases: pharmacological data and clinical evidence [J]. *Oxid Med Cell Longev*, 2021, **2021**: 6678662.
[49] Li Q, Tan JX, He Y, *et al*. Atractylenolide III ameliorates nonalcoholic fatty liver disease by activating hepatic adiponectin receptor 1-mediated AMPK pathway [J]. *Int J Biol Sci*, 2022, **18**(4): 1594-1611.
[50] Fan Y, Dong W, Wang Y, *et al*. Glycyrrhetinic acid regulates impaired macrophage autophagic flux in the treatment of non-alcoholic fatty liver disease [J]. *Front Immunol*, 2022, **13**: 959495.

Cite this article as: WU Yuanyuan, ZHOU Jingwen, ZUO Xinchen, KUANG Yufeng, SUN Lixia, ZHANG Xiaolong. Yanggan Jiangmei Formula alleviates hepatic inflammation and lipid accumulation in non-alcoholic steatohepatitis by inhibiting the NF-*κ*B/NLRP3 signaling pathway [J]. *Chin J Nat Med*, 2024, **22**(3): 224-234.